

# Synthesis of a DNA Knot Containing Both Positive and Negative Nodes

Shou Ming Du and Nadrian C. Seeman\*

Contribution from the Department of Chemistry, New York University,  
New York, New York 10003. Received February 5, 1992

**Abstract:** A figure-eight ( $4_1$ ) knot, containing two positive and two negative nodes, has been synthesized by ligating a single-stranded DNA molecule into a closed cycle. The molecule consists of two single-turn double-helical domains connected by four  $dT_{14}$  or  $dT_{15}$  linkers. One of the domains contains the sequence  $(dCpdGp)_6$ , which is capable of forming left-handed Z-DNA. Ligation yields a trefoil ( $3_1$ ) knot or a  $4_1$  knot, depending upon the conditions in solution. A  $4_1$  knot results if  $Co(NH_3)_6^{3+}$  is present in the solution to promote the formation of Z-DNA; a  $3_1$  knot is the product in the absence of  $Co(NH_3)_6^{3+}$ . Both domains of the  $3_1$  knot are susceptible to restriction endonuclease digestion, but only the domain of the  $4_1$  knot expected to be right-handed can be digested by a restriction endonuclease. The  $4_1$  knot has both a higher gel-electrophoretic mobility at low polyacrylamide concentrations and a higher friction constant than the  $3_1$  knot, when analyzed by Ferguson plots under denaturing conditions.

## Introduction

The knotting of DNA molecules is a prominent phenomenon. Living cells contain topoisomerases that can perform strand passage operations on single-stranded<sup>1</sup> or double-stranded<sup>2</sup> DNA to knot<sup>1,3</sup> or unknot<sup>2,4,5</sup> the molecules. In addition to topoisomerases, site-specific recombination systems are capable of forming knotted DNA molecules: The integration system of bacteriophage  $\lambda$ ,<sup>6-8</sup> the  $\mu$ ,<sup>9</sup> Gin,<sup>10</sup> and Hin<sup>11</sup> transposition apparatus; and the transposon Tn3 resolvase<sup>12,13</sup> are examples of site-specific recombination systems whose modes of action have been analyzed by examination of the knotted products of their action. RNA pseudoknots<sup>14-16</sup> are a related biological motif, but they lack the braiding interactions of true knots.

Beyond the biological realm, knots have been a concern of chemical topology at least since Frisch and Wasserman proposed their existence in polymers 30 years ago.<sup>17</sup> Attempts to achieve deliberate knotting in small molecular systems have been made by numerous investigators;<sup>18,19</sup> this goal has been achieved recently by Sauvage and his colleagues.<sup>20,21</sup> Synthetic schemes for constructing knotted molecules are not predicated on the enzymatic strand passage strategy used by the living cell. Rather, they rely on the ability to braid deliberately one part of the molecule about another.

It is not necessary to depend on strand passage enzymes to form knotted single-stranded DNA molecules. Indeed, the plectonemic nature of double-helical DNA makes it an ideal molecule to use in forming chemical knots by means of deliberate braiding. It is easy to include Watson-Crick pairing sequences that generate double helices within a linear molecule, in order to produce the braiding sought. For example, we have reported recently the synthesis of a trefoil ( $3_1$ ) knot from single-stranded DNA.<sup>22</sup> This knot is a cyclic 104-mer, with the sequence A-T-B-T-A'-T-B'-T, where A and B represent 11 nucleotides complementary to A' and B', respectively, and T represents a  $dT_{15}$  segment. The paired A and B regions form double-helical domains, and the T segments are single-stranded spacers between them.

When a knotted object is projected onto a plane, the figure contains nodes where the curve crosses itself. If the curve is given an arbitrary directionality along its length, nodes of two senses, positive and negative, may arise. Naturally occurring B-DNA is right-handed, and right-handed helices generate topologically negative nodes, as shown in Figure 1. Hence, the DNA knot we reported earlier corresponds to the topological enantiomer containing negative nodes.<sup>22</sup> Many knots contain mixtures of positive and negative nodes, so it is desirable to be able to create them in DNA molecules. Fortunately, DNA can exist in a left-handed

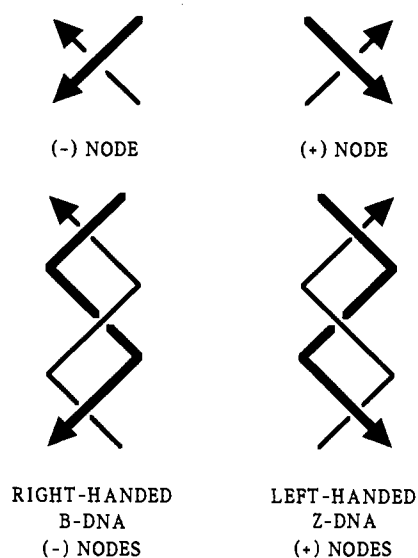


**Figure 1.** Nodes and DNA handedness. The upper part of this drawing shows positive and negative nodes, with their signs indicated. It is useful to think of the arrows as indicating the 5'  $\rightarrow$  3' direction of the DNA backbone. Below the negative node is a representation of about one and one-half turns of a right-handed B-DNA molecule. Note that the nodes are all negative. Below the positive node is a left-handed Z-DNA molecule. Note that the nodes are all positive. The Z-DNA molecule has been drawn so as to appear to be a left-handed version of B-DNA. This has been done to clarify the relationship between the handedness of a double helix and the signs of the nodes generated. *This drawing is not intended to represent accurately the structural nature of the Z-DNA helix, in which the minor groove is less exposed than in the B-DNA helix, the major groove is nonexistent, and the backbone has a zig-zag character.*<sup>23</sup>

structure, Z-DNA, which, in principle, enables one to introduce positive nodes into a DNA knot (Figure 1). In order to do so, one must select a sequence amenable to forming Z-DNA and then perform the ligation under conditions that promote the Z-DNA<sup>23-25</sup> structure.

(1) Liu, L. F.; Depew, R. E.; Wang, J. C. *J. Mol. Biol.* **1976**, *106*, 439-452.

(2) Mizuuchi, K.; Fisher, L. M.; O'Dea, M. H.; Gellert, M. *Proc. Natl. Acad. Sci. U.S.A.* **1980**, *77*, 1847-1851.

(3) Dean, F. B.; Stasiak, A.; Kollmer, T.; Cozzarelli, N. R. *J. Biol. Chem.* **1984**, *260*, 4975-4983.

(4) Liu, L. F.; Liu, C.-C.; Alberts, B. M. *Cell* **1980**, *19*, 697-707.

(5) Shishido, K.; Komiyama, N.; Ikawa, S. *J. Mol. Biol.* **1987**, *195*, 215-218.

\* To whom correspondence should be addressed.

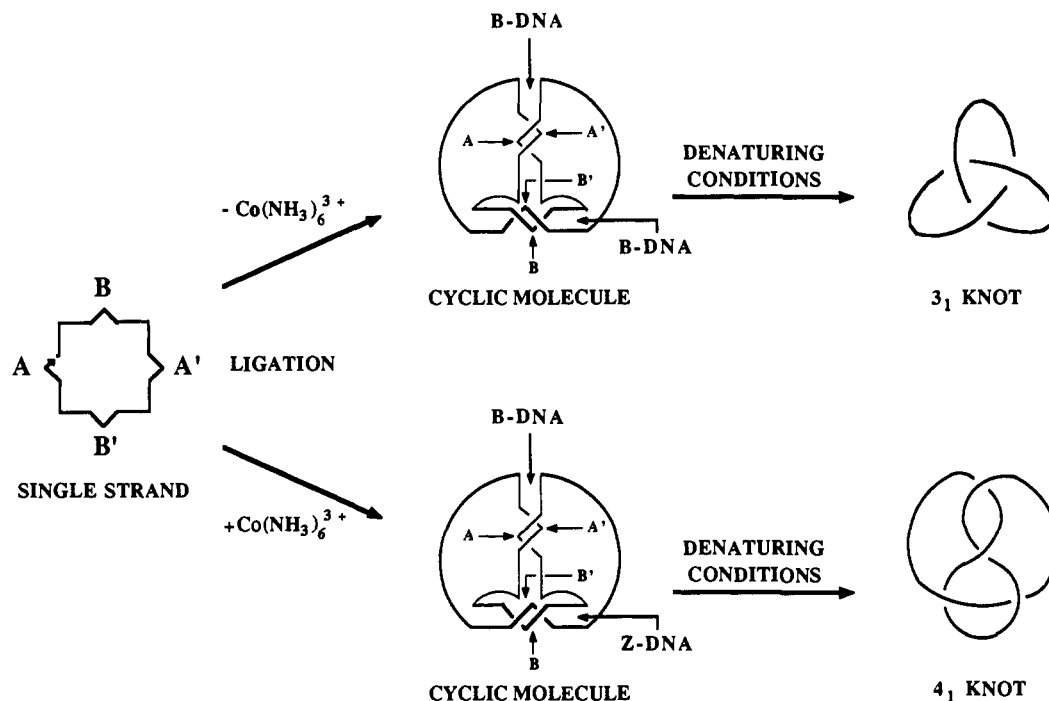


**Figure 2.** Synthetic scheme for the single-stranded DNA knots. The starting material is the 104-mer illustrated on the far left.  $A = (A-C-T-G-G-A-C-C-T-C-T)$ ,  $B = (dCpdGp)_6$ , and  $A'$  and  $B'$  refer to sequences that are expected to pair to  $A$  and  $B$  by Watson-Crick hydrogen bonding. Each side of the square figure shown corresponds to a quarter of the molecule. The projections represent the regions that will pair according to the letter codes; they are flanked by the oligo(dT) linkers. The arrowhead within the  $A$  projection represents the 3' end of the strand. There are two routes to the structures shown in the central portion of the figure: the bottom route, including the addition of Z-promoting  $Co(NH_3)_6^{3+}$ , and the top route, without  $Co(NH_3)_6^{3+}$ . The central section of the figure represents a version of the molecule distorted from its expected structure, in order to illustrate the interlinking of the strands. The regions corresponding to the left part of the figure are indicated. The double-helical linking is concentrated in one portion of each helical domain, for clarity.<sup>32</sup> Both helices are viewed from the minor-groove side at the middle. The expected B or Z structures are indicated for each domain. The oligo(dT) linkers are represented here by the curved portions of the strand; two have been enlarged, and two have been shrunk, to place the vertical helix in a position where it is unoccluded by the horizontal one. The vertical helix is further from the viewer than is the horizontal one, as indicated by its lighter lines. The upper right drawing illustrates the denatured trefoil structure in an idealized fashion. Note that the handedness of the trefoil shown here is the correct one for right-handed double-helical DNA. The lower right drawing represents the  $4_1$  knot similarly. Note that reversing the sense of all the nodes of this knot results in no change in handedness, as this knot is amphichiral.<sup>7</sup>

Here we report the construction of a knot containing both positive and negative nodes. The same A-T-B-T-A'-T-B'-T cyclic pairing motif used earlier will generate the figure-eight ( $4_1$ ) knot if the nodes in one of the helical domains are positive and the nodes in the other domain are negative. Accordingly, we have replaced each side of the undecamer B-B' domain of the  $3_1$  knot<sup>22</sup> with the dodecamer sequence  $(dCpdGp)_6$ , which is capable of forming Z-DNA. We promote the B-Z transition by adding  $Co(NH_3)_6^{3+}$ , which is convenient<sup>26</sup> for enzymatic ligation. This is the first time that a chemical  $4_1$  knot has been assembled deliberately. This

knot is termed amphichiral, because the same knot is obtained when the signs of its two positive nodes and two negative nodes are reversed.<sup>7</sup>

## Materials and Methods

**Synthesis and Purification of DNA.** All DNA molecules in this study were synthesized on an Applied Biosystems 380B automatic DNA synthesizer, removed from the support, and deprotected, using routine phosphoramidite procedures.<sup>27</sup> Molecules were synthesized with a 5' phosphate added chemically, using 2-[[2-[(4,4'-dimethoxytrityl)oxy]ethyl]sulfonyl]ethyl 2-cyanoethyl *N,N*-diisopropylphosphoramidite from Glen Research (Sterling, VA). DNA strands were purified by denaturing gel electrophoresis.

**Enzymatic Reactions. A. Kinase Labeling.** Two picomoles of an individual strand of DNA was dissolved in  $10 \mu\text{L}$  of a solution containing 66 mM Tris-HCl, pH 7.6, 6.6 mM  $MgCl_2$ , and 10 mM dithiothreitol (DTT) and mixed with  $1 \mu\text{L}$  of  $2.2 \mu\text{M}$  [ $\gamma$ - $^{32}\text{P}$ ]ATP (10 mCi/mL) and 5 units of polynucleotide kinase (Boehringer) for 2 h at 37 °C. The reaction was stopped by heating the solution to 90 °C. We find that previous chemical phosphorylation results in increased specific activity of the radioactively labeled material, because no chase reaction with unlabeled ATP is necessary.

(6) Griffith, J. D.; Nash, H. A. *Proc. Natl. Acad. Sci. U.S.A.* **1985**, *82*, 3124-3128.

(7) Wasserman, S. A.; Cozzarelli, N. R. *Science* **1986**, *232*, 951-960.

(8) Spengler, S. J.; Stasiak, A.; Cozzarelli, N. R. *Cell* **1985**, *42*, 325-334.

(9) Craigie, R.; Mizuuchi, K. *Cell* **1986**, *45*, 793-800.

(10) Kanaar, R.; van de Putte, P.; Cozzarelli, N. R. *Cell* **1989**, *58*, 147-159.

(11) Heichman, K. A.; Johnson, R. C. *Science* **1990**, *249*, 511-517.

(12) Wasserman, S. A.; Dungan, J. M.; Cozzarelli, N. R. *Science* **1985**, *229*, 171-174.

(13) Gellert, M.; Nash, H. *Nature* **1987**, *325*, 401-404.

(14) Schimmel, P. *Cell* **1989**, *58*, 9-12.

(15) Pleij, C. W. A. *Trends Biochem. Sci.* **1990**, *15*, 143-147.

(16) Puglisi, J. D.; Wyatt, J. R.; Tinoco, I. *Acc. Chem. Res.* **1991**, *24*, 142-158.

(17) Frisch, H. L.; Wasserman, E. *J. Am. Chem. Soc.* **1961**, *83*, 3789-3795.

(18) Walba, D. M. *Tetrahedron*, **1985**, *41*, 3161-3212.

(19) Sauvage, J.-P. *Acc. Chem. Res.* **1990**, *23*, 319-327.

(20) Dietrich-Buchecker, C. O.; Sauvage, J.-P. *Angew. Chem., Int. Ed. Engl.* **1989**, *28*, 189-192.

(21) Dietrich-Buchecker, C. O.; Guilhem, J.; Pascard, C.; Sauvage, J.-P. *Angew. Chem., Int. Ed. Engl.* **1990**, *29*, 556-557.

(22) Mueller, J. E.; Du, S. M.; Seeman, N. C. *J. Am. Chem. Soc.* **1991**, *113*, 6306-6308.

(23) Wang, A. H.-J.; Quigley, G. J.; Kolpak, F. J.; Crawford, J. L.; van Boom, J. H.; van der Marel, G.; Rich, A. *Nature* **1979**, *282*, 680-686.

(24) Pohl, F. M.; Jovin, T. M. *J. Mol. Biol.* **1972**, *67*, 375-396.

(25) Rich, A.; Nordheim, A.; Wang, A. H.-J. *Annu. Rev. Biochem.* **1984**, *53*, 791-846.

(26) Behe, M.; Felsenfeld, G. *Proc. Natl. Acad. Sci. U.S.A.* **1981**, *78*, 1619-1623.

(27) Caruthers, M. H. In *Chemical and Enzymatic Synthesis of Gene Fragments*; Gassen, H. G., Lang, A., Eds.; Verlag Chemie: Weinheim, 1982; pp 71-79.

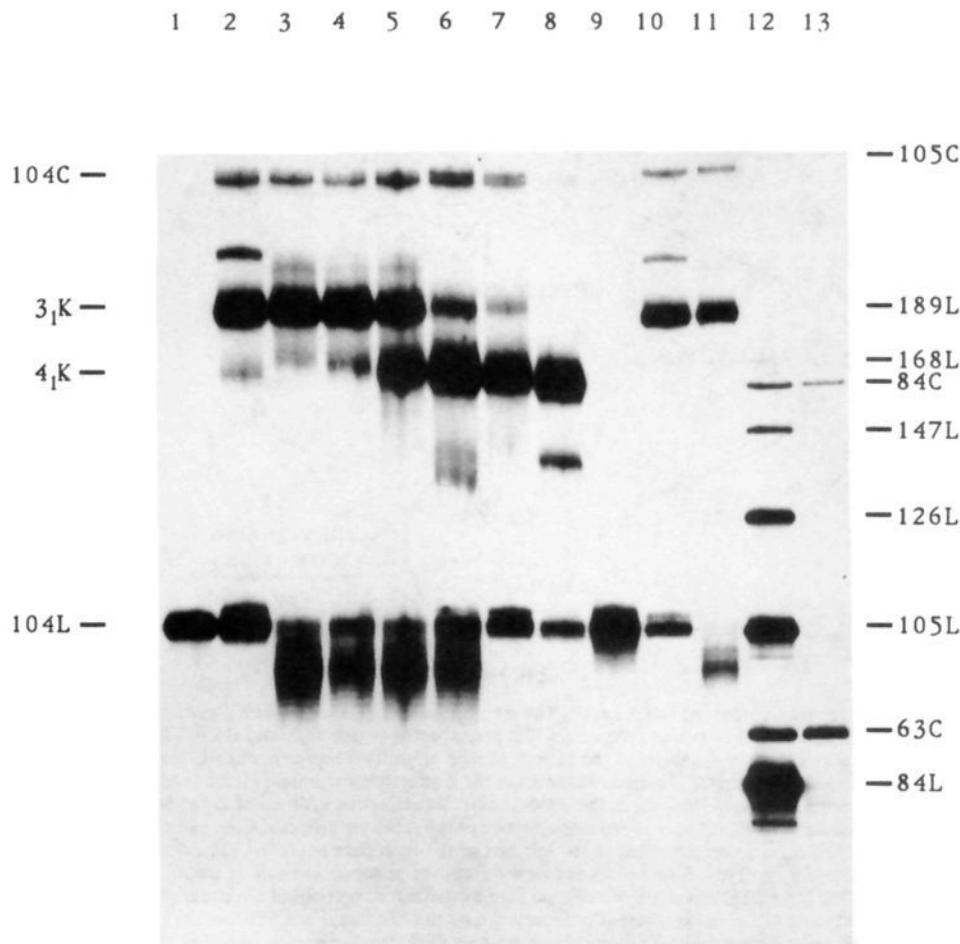


**Figure 3.** Synthesis and characterization of the  $4_1$  knot. This is an autoradiogram of a denaturing 10% polyacrylamide gel containing the ligation and digestion products of the 104-mer species. Lanes 10–13 contain electrophoretic size standards for comparison with the experimental lanes, 1–9. Lane 10 contains the products of treating with T4 DNA ligase the previously reported  $3_1$  knot-producing strand,<sup>22</sup> and lane 11 contains the exonuclease III digestion products of the material in lane 10. Lanes 12 and 13 contain linear (L) and circular (C) length markers generated by ligating a three-arm DNA branched junction containing 21 nucleotide pairs between vertices;<sup>22</sup> lane 13 contains the exonuclease III digestion products of the material in lane 12. Bands corresponding to the linear (L) reactant and circular (C) and knotted (K) products of the current construction are indicated on the left side of the figure. Lane 1 contains the unligated strand reported herein, lane 2 contains its ligation products, and lane 3 contains the same strand subjected to both ligation and exonuclease III. Compare the major exonuclease III-resistant band in lane 3 with the knot in lane 11, and the slower-moving, exonuclease III-resistant band with the 105-mer circle in lane 13. Lanes 4, 5, and 6 contain the same strand ligated and exonuclease III-treated in the presence of 0.1, 1.0, and 10 mM  $\text{Co}(\text{NH}_3)_6^{3+}$ , respectively. Note the emergence of the more rapidly moving band in response to the presence of  $\text{Co}(\text{NH}_3)_6^{3+}$ . Lane 7 contains the same strand ligated in the presence of 10 mM  $\text{Co}(\text{NH}_3)_6^{3+}$ , but not treated with exonuclease III. Lanes 8 and 9 contain material like that in lane 7 except that it has been ligated in the presence of 3 mM  $\text{Co}(\text{NH}_3)_6^{3+}$ . In addition, the material in lane 8 has been treated with *HhaI* (cleavage site GCGC), and the material in lane 9 has been treated with *Sau96I* (cleavage site GGNCC). Note that only the  $3_1$  knot is digested after treatment with *HhaI*, but that both knots are sensitive to treatment with *Sau96I*, suggesting that the  $(\text{dCpdGp})_6$  domain contains a conformation that is not sensitive to digestion.

**B. Ligations.** Ligations were performed in the kination buffer, which was brought to 66  $\mu\text{M}$  ATP. Ten units of T4 polynucleotide ligase (U.S. Biochemical) was added, and the ligation proceeded at 16 °C for 10–16 h.  $\text{Co}(\text{NH}_3)_6\text{Cl}_3$  (Aldrich) was added to ligations for which the  $4_1$  knot was the target molecule. The reaction was stopped by phenol/chloroform extraction. Samples to be restricted were ethanol precipitated.

**C. Restriction Endonuclease Digestions.** Restriction enzymes were purchased from New England Biolabs and used in buffers suggested by the supplier. Digestion was performed at 37 °C for 2 h with 20 units of *HhaI* or *Sau96I*.

**D. Exonuclease III Treatment.** One hundred units of exonuclease III (U.S. Biochemical) was added directly to the ligation mixture, and the reaction was allowed to proceed for 2 h at 37 °C.

**Denaturing Polyacrylamide Gel Electrophoresis.** Gels contained 8.3 M urea and 10% acrylamide (19:1 acrylamide/*N,N'*-methylenebis(acrylamide)). The running buffer consisted of 89 mM Tris-HCl, pH 8.0, 89 mM boric acid, and 2 mM EDTA (TBE). The sample buffer consisted of 10 mM NaOH and 1 mM EDTA containing 0.1% Xylene Cyanol FF tracking dye. Gels were run on an IBI Model STS 45 electrophoresis sequencing gel unit at 70 W (50 V/cm) constant power, dried onto Whatman 3MM paper, and exposed to Kodak X-OMAT AR film for up to 15 h. For Ferguson analysis, denaturing gels were run at 63.5

°C on a Hoefer SE 600 electrophoresis unit. Absolute mobilities (cm/h) were measured, and logarithms were calculated to base 10.

## Results

Figure 2 indicates the synthetic scheme used to construct the  $4_1$  knot. Each pairing region is separated by a  $\text{dT}_{14}$  or  $\text{dT}_{15}$  spacer. The 5' and 3' ends of the synthetic molecule fall between the eighth and ninth nucleotides of the A segment, producing a nick that can be sealed by T4 DNA ligase. Ligation in B-promoting conditions is expected to produce a  $3_1$  knot (Figure 2, top); ligation in Z-promoting conditions is expected to generate a  $4_1$  knot (Figure 2, bottom). We characterize the products under denaturing conditions, which are sensitive to topology, regardless of molecular conformation.<sup>22,28</sup>

The results of ligation are illustrated in Figure 3. Lane 1 contains unligated material, lane 2 contains material treated with T4 DNA ligase under B-promoting conditions, and lane 3 contains

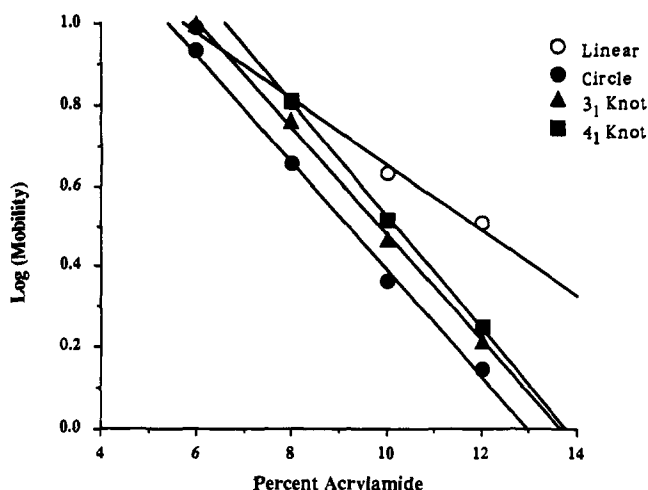


**Figure 4.** Ferguson plot of the 104-mer DNA molecule as a linear molecule, a circle, a  $3_1$  knot, and a  $4_1$  knot. The negative slopes of the plots are 0.081, 0.132, 0.132, and 0.140 for the linear molecule, the circle, and the  $3_1$  and  $4_1$  knots, respectively. The intercepts are 1.46, 1.71, 1.79, and 1.92 for the same molecules. The measuring error is about  $\pm 0.5$  mm, or  $\pm 0.033$  cm/h. This converts to a spread for the slopes of the  $3_1$  and  $4_1$  knots of 0.130–0.134 and 0.139–0.144, respectively, so that the difference between them is significant. It is important to remember that the relative mobilities of molecules will interchange if their Ferguson plots intersect.

the same ligated material treated with exonuclease III. The prominent products in these lanes are the  $3_1$  knot and the circle of the same sequence. The previously characterized  $3_1$  knot of the same length<sup>22</sup> is shown in lanes 10 and 11, and linear and cyclic markers<sup>22</sup> are shown in lanes 12 and 13. Lanes 4, 5, and 6 show the products of ligating the material in the presence of 0.1, 1.0, and 10 mM  $\text{Co}(\text{NH}_3)_6\text{Cl}_3$ , respectively. The material in each of these lanes was treated with exonuclease III. The intensity of the band corresponding to the  $3_1$  knot decreases with increasing concentrations of  $\text{Co}(\text{NH}_3)_6\text{Cl}_3$ ; simultaneously, a faster-moving band appears. Single-stranded<sup>22</sup> and double-stranded<sup>3,29</sup> DNA knots of greater complexity are known to migrate more rapidly than DNA circles or less complex knots of the same length. Therefore, we ascribe the new product to the  $4_1$  knot. The previously reported  $3_1$  knot-producing strand of the same length<sup>22</sup> lacks a sequence that can form Z-DNA readily; the products of ligating this molecule in the presence or absence of 1 mM  $\text{Co}(\text{NH}_3)_6\text{Cl}_3$  are identical and lack the band corresponding to the  $4_1$  knot (data not shown).

The A domain contains a *Sau96I* restriction endonuclease site, and the B domain contains four *HhaI* sites. Lane 7 of Figure 3 contains the same material as lane 6, except that it was not treated with exonuclease III. The material in lanes 8 and 9 was treated with 3 mM  $\text{Co}(\text{NH}_3)_6^{3+}$  prior to ligation and was not treated with exonuclease III. Lane 8 contains the results of digesting the

ligation products with *HhaI*: The circle and the  $3_1$  knot were digested, but the putative  $4_1$  knot remained intact. Lane 9 contains the results of treating the ligation products with *Sau96I*: the circle,  $3_1$  knot, and  $4_1$  knot were all digested by this enzyme. Thus, the right-handed domains on both knots are digested, but one domain in the  $4_1$  knot is resistant to digestion, suggesting that it is left-handed.

Ferguson analysis<sup>30</sup> provides a means of distinguishing the properties of molecules in a gel. The logarithm of the mobility is plotted as a function of polyacrylamide concentration; the resulting slope is proportional to the friction constant of the molecule. As seen in Figure 4, the  $4_1$  knot has a higher friction constant than the  $3_1$  knot of the same sequence under denaturing conditions. The slope of the plot for the  $4_1$  knot is about 5% greater than that for the  $3_1$  knot. The two plots intersect at approximately 16% acrylamide. This suggests that the presence of more nodes per unit length results in a higher friction constant. Note that the higher mobility of the  $4_1$  knot at low acrylamide concentrations is likely to result from its greater compactness. The friction constant of this  $3_1$  knot is the same as that of the circle, although the friction constant of the previously reported  $3_1$  knot is about 9% higher than that of its corresponding circle.<sup>22</sup> The two  $3_1$  knots migrate similarly on these gels; it is the circle that appears to have a higher friction constant than the previous circle (data not shown).

## Discussion

We have demonstrated that it is possible to construct a knot from DNA that contains both positive and negative nodes. The positive nodes are introduced into the molecule by including a sequence that forms Z-DNA readily, followed by enzymatic ligation under gentle Z-forming conditions. The ability to form knots containing nodes of both signs vastly increases the number of different knots that may be engineered from single-stranded DNA. In addition, both topological enantiomers of many chiral knots are now available. The general design of knotted molecules from single-stranded nucleic acids will be discussed elsewhere.

The ligation of the  $4_1$  knot under Z-promoting conditions proceeds as readily as the ligation of the  $3_1$  knot under conventional conditions. However, if the Z-forming sequence used,  $(\text{dCpdGp})_6$ , were the only Z-forming sequence available, it would be hard to engineer complex knots with Z domains: The fidelity of pairing in the desired fashion would be problematical because of the large amount of sequence symmetry.<sup>31</sup> Fortunately, there are numerous sequences that will convert to the Z form under appropriate conditions.<sup>25</sup> Thus, the synthesis of knots incorporating multiple domains that contain positive nodes appears to be feasible.

**Acknowledgment.** We are grateful to Dr. Nicholas Cozzarelli for providing us with a copy of the program Knotter by John Jenkins. This research has been supported by Grant GM-29554 from the NIH. The support of Biomolecular Imaging on the NYU campus by the W. M. Keck Foundation is gratefully acknowledged.

(30) Rodbard, D.; Chrambach, A. *Anal. Biochem.* **1971**, *40*, 95–134.

(31) Seeman, N. C. *J. Theor. Biol.* **1982**, *99*, 237–247.

(32) Chen, J.-H.; Kallenbach, N. R.; Seeman, N. C. *J. Am. Chem. Soc.* **1989**, *111*, 6402–6407.

(29) White, J. H.; Millett, K. C.; Cozzarelli, N. R. *J. Mol. Biol.* **1987**, *197*, 585–603.